# SILICON ETCHING IN LAPPS

*Abstract*

Initial tests using LAPPS to etch silicon with sulfur hexafluoride containing plasmas were carried out. Material removal rates and anisotropy were determined with respect to gas composition and substrate rf-induced self-bias level. At room temperature, the removal rate increased linearly with substrate bias. Mixtures of argon and sulfur hexafluoride etched approximately ten times faster (5000 Å/min) than similar mixtures of oxygen/sulfur hexafluoride (~500 Å/min), with the difference being attributed to the passivation of the silicon by involatile silicon oxyfluoride ($SiO_xF_y$) compounds. At low incident ion energies, these involatile species are believed to cause the observed tapered feature profiles, which became more vertical with increasing ion energy. Plasma and surface chemistry are also discussed, including the negative ion character of these plasmas.

## 1. INTRODUCTION

Silicon etching has been considered "one of the most understood and most widely used plasma process"[1] yet continues to evolve as more applications are found. Applications such as gate oxide etching in electronic devices require shallow etches with small (0.1 micron) features while deep, micron-sized features are desired for micro-electro mechanical (MEMS) devices. This large feature etching has caused a resurgence in plasma processes using sulfur hexafluoride, due to its low toxicity and the large amount needed for bulk material removal. To control the feature evolution in these applications, intermittent deposition (or passivation) steps are used to coat the feature sidewalls and inhibit unwanted undercutting.[2] These deposition-etch processes can furthermore be done at room temperature, as opposed to relying on cryogenic temperatures to inhibit the chemical (isotropic) etch component of the process. While fluorocarbon species are generally used for the passivation cycles, anisotropic etching of silicon has been done in $O_2/SF_6$ mixtures[3,4,5] with the oxygen also passivating feature sidewalls. These mixtures vary widely in composition (0-50% $O_2$) and etch rate (200-2000 nm/min) with no obvious correlation.

The Large Area Plasma Processing System (LAPPS) developed at NRL has been studied and discussed experimentally in Reference [6]. The system uses a sheet electron beam (e-beam) to ionize background gas, which results in high-density plasmas with very cold plasma electron distributions and low internal electric fields. In this series of experiments, typical reactive ion etch conditions were applied to this plasma source to determine the process viability. The studies presented are considered to be complete but preliminary and by no means comprehensive.

### *1.1. Silicon Etching*

Silicon etching in fluorine-containing plasmas is carried out through the formation of the volatile $SiF_4$ species and liberation of $SiF_2$ radicals from the surface. The reactive species is atomic fluorine[i] formed in the gas phase. The fluorine atoms individually break Si-Si bonds (initially from the underside of the surface atom) to form the volatile $SiF_4$ product. Focusing on $SF_6$ chemistries, in the gas phase four fluorine atoms are liberated by the dissociation process $SF_6 + e^- \rightarrow SF_2 + 4F + e^-$ ($k_d \sim 58\ s^{-1}$). This reaction and the general low toxicity of $SF_6$ make it an attractive processing gas. Adding small amounts of oxygen to the process gas results in reactive atomic oxygen, which has a number of effects[ii] on both gas phase and surface chemistry: (1) breaks double bonds in polymer-forming species to prevent surface passivation; (2) forms $SiO_2$ on Si surface, which slows etching; (3) burns $SF_2$ radicals, forming SOF, $SOF_2$, $SO_2F_2$ as well as $SO_2$; and (4) burns fluorocarbon radicals, forming $CO_xF_y$ when carbon is present. All of these reactions have both positive and negative effects that have been discussed in the literature. In this work, we will primarily consider effects (2) and (3). Effect (2), the formation of $SiO_2$, can be used to passivate feature sidewalls and assist process anisotropy, particularly in MEMS devices, where the exposed surfaces eventually become oxidized. The problem is that atomic O passivates all surfaces at comparable rates. This means that higher ion energies will be necessary to remove the thin $SiO_2$ layer on the surface being etched, which may be undesirable. Effect (3), the burning of $SF_2$ radicals, is considered attractive because $SF_2$ acts as a getter of the reactive F atoms

[i] To some extent, molecular as well.
[ii] We will not consider any global plasma changes in electron temperature or plasma potential.

through the reaction $SF_x + F \rightarrow SF_{x+1}$. In conventional discharges, low concentrations of oxygen (< 10% [$O_2$]) increased F atom concentrations ([F]) by greater than a factor of 2, competing with the $SF_x$ recombination through chain reactions such as $SF_2 \rightarrow SOF \rightarrow SOF_2 \rightarrow SO_2$. At higher [$O_2$], the increased [O] dominates the reactions with $SF_2$, consuming the $SF_2$ at nearly the $SF_6$ dissociation rate, but also increases the probability of forming $SiO_2$ on the Si surface. While LAPPS differs from conventional discharges, the same gas-phase neutral reactions occur, so an accurate depiction of plasma chemistry is still vital.

### *1.2. Negative Ions and Ion-Ion Plasmas*

'Ion-ion' plasmas form when plasma electrons attach to an electronegative species in large quantities such that atomic or molecular anions, not the plasma electrons, are the primary negative charge carriers. Typically, the phrase 'ion-ion plasma' refers to a state where the negative ion density is 100-1000 times that of the electron density. Such a large imbalance of negative charge carriers is necessary before the plasma character actually changes, since the plasma electrons respond more rapidly to external influences. Because electron-attachment to halogen gases typically favors low-energy electrons, studies of ion-ion plasmas in conventional discharges have been limited to afterglows or remote plasma sources, where electron temperatures are low. However, electron beam produced plasmas are ideal for generating ion-ion plasmas with $SF_6$; LAPPS with any molecular gas produces extremely low electron temperatures (< 0.5 eV), and the attachment rate for low energy electrons to $SF_6$ increases exponentially[7] as electron temperatures fall below 0.5 eV.

Negative ions have been studied as strong candidates to neutralize charge build up in silicon processing. Initially, modulated etching plasmas (which contain electronegative gases) alleviated notching issues[8] associated with electron charge buildup on insulated surfaces, by allowing the charge to dissipate between pulses. A low frequency (600 kHz) rf bias was claimed to provide better directional etching[9] when negative ions were used in place of electrons to neutralize the charge deposited by positive ions. In this work, we take a preliminary look at the negative ion character of

modulated $SF_6$-containing plasmas generated by e-beam ionization and the effects of standard rf biasing on silicon etching.

## 2. EXPERIMENTAL SETUP

### *2.1. Plasma Chamber and Cathode Operation*

The cathode used to generate the e-beam and the entire chamber has been discussed previously.[10] This system consisted of a brass hollow cathode with Telfon® insulation and powered by a high voltage (-2 kV) square-wave pulse in a cylindrical (40 cm diameter) acrylic chamber. A slotted anode located 5 cm in front of the cathode defined the beam cross section (25 cm x 1 cm), with a beam dump anode located ~ 30 cm downstream. The cathode was located on the chamber axis and centered within a set of independently supported Helmholtz coils. A base vacuum in the $10^{-4}$ torr range was provided with a 25 l/s turbomolecular pump, while gas flow was provided by a combination of Leybold leak valves and throttling the turbo pump with a manual butterfly valve. Operating pressures were monitored by a MKS capacitance manometer[i] and a Convectron® gauge. At magnetic fields of 75-200 G, this hollow cathode usually operated in a 'high impedance' mode.[11] A fixed duty factor of 10% was used in all experiments.

### *2.2. Etching Stage and Rf Biasing*

The etching stage consisted of a stainless steel front plate (~ 7 cm diameter, 2 mm thick) insulated by Telfon® sheet (5 mm thick) from a grounded support structure. The front plate contained four tapped holes on a 3.8 cm bolt circle to fasten the sample carriage to the stage. The sample carriage was a small stainless steel plate (0.75 mm thick) with slots around the perimeter to accommodate the stage mounting screws, which allowed rapid sample changes (via multiple carriages). Samples were typically adhered to the carriage with silver print epoxy. The support structure was an aluminum block, mounted on an optical mounting post and platform. The aluminum block held the powered electrode and housed the power connection. The platform was fastened to the

[i] The capacitance manometer frequently gave false readings while the cathode was running, so the Convectron gauge was used to monitor any gross changes in chamber pressure during long processing runs.

beam dump anode for mechanical stability and reproducible positioning. A few layers of Telfon® tape were wrapped around the perimeter of the stainless steel plate and were held in place with an outer wrap of copper tape, which also contacted the aluminum block. A coaxial cable (RG174) was run from the stage to an isolated vacuum feedthrough to reduce grounding problems between the rf power supply, stage and the rest of the system. This internal cable was stripped of its outer insulation jacket exposing the ground braid, to reduce outgassing due to trapped air.

The rf power was applied to the stage through a pick-off box[i] by a commercial capacitive matchbox ('pi' configuration) in series with a rf power amplifier and laboratory signal generator. To minimize erroneous results from unwanted rf discharges, the rf power was applied only when the e-beam pulse was present, after a brief delay (100-200 μs) to avoid any transient ignition behavior from the cathode. Matching or coupling of the applied rf voltage to the plasma was considered to be ideal when the rf signal amplitude and dc offset (see below) were at a maximum during the beam pulse as measured in the pick-off box. The external measurements made at the pick-off box are not necessarily the signal values at the stage surface but provide relative values for the rf currents, voltages and rf-induced dc bias (or just 'rf bias'). The rf bias is the average voltage induced on the stage and it is indicative of the impinging ion energy. Technically, the ion energy is the difference in the plasma potential and the measured rf bias. In LAPPS, the plasma potential is low (≤ 3 V in these experiments) and was considered to be negligible, given the rf bias levels used. Following convention, only the rf bias ($V_{bias}$) is reported here, as the plasma potentials were not actively measured.

The rf bias capabilities of the stage were similar to stages discussed previously.[10] Initially, differences in stage performance were attributed to minor design changes, but tests performed after the etching experiments showed that the observed differences were in fact due to the acrylic chamber. Specifically, with the stage floating, a persistent –15 V signal was measured during the e-beam pulse. For the etching experiments, this constant [negative] offset voltage was always present and included in the rf-induced dc bias level. Hence, -50 V bias voltages were achieved with peak-to-peak rf voltages as

[i] The box housed a small (1V/A) Pearson coil that enclosed the main power feed to measure current flow and a standard 10X oscilloscope probe which allowed a consistent reading of the voltage. The box was placed inline at the stage power feedthrough, outside the vacuum system.

low as 44 to 50 V. After weeks of heavy use and then sitting dormant, the dc signal rose to more than -60 V. When the stage was then placed into a metal chamber with a base pressure < $5x10^{-7}$ torr, a smaller negative signal was seen during the e-beam pulse. As the cathode was run at typical processing conditions, this signal rapidly decreased to zero, then to a steady-state value of +1.25 V over the course of a few minutes.

### *2.3. Typical etching conditions*

'Typical' etching conditions pertain to the cathode operating at a 10% duty factor with a –2 kV pulse in a magnetic field. For the $O_2/SF_6$ mixtures, an 83 Gauss field was applied and the high voltage pulse was set at 5 ms width with a 20 Hz repetition rate. For the $Ar/SF_6$ mixtures, a 90 Gauss field was applied with a 2 ms/50 Hz high voltage pulse. Operating pressures varied slightly with gas composition to keep the cathode operation stable. The front surface of the etching stage was positioned ≈ 1 cm from the e-beam edge as defined by the slotted anode. Rf biasing was achieved by tuning the rf matchbox and increasing the rf amplitude until a desired dc offset ($V_{bias}$) was obtained. Setting the ion energy in this manner was straightforward, but contained systematic problems as discussed in Section 2.2. Tables I and II show rf signal values for various rf bias levels for $SF_6$ mixtures with Ar and $O_2$ in the acrylic chamber.

**Table I Peak-to-peak voltages and currents for various bias voltages measured with 50 mtorr Ar and 20 mtorr $SF_6$ mixture.**

| $V_{bias}$(V) | $V_{p-p}$(V) | $I_{p-p}$(A) |
|---|---|---|
| -32 | 18 | 0.5 |
| -50 | 60 | 2.1 |
| -75 | 92 | 2.8 |
| -100 | 130 | 3.86 |
| -200 | 272 | 8.09 |

**Table II Peak-to-peak voltages and currents for various bias voltages measured with 45 mtorr $O_2$ and 15 mtorr $SF_6$ mixture.**

| $V_{bias}$(V) | $V_{p-p}$(V) | $I_{p-p}$(A) |
|---|---|---|
| -50 | 38 | 2.7 |
| -75 | 56 | 4.1 |
| -100 | 78 | 5.5 |
| -150 | 117 | 7.85 |
| -200 | 156 | 9.72 |

### *2.4. Samples*

Single crystal silicon wafers (<110>) were cut into ≈ 1 $cm^2$ pieces and masked with silver print epoxy, which was fairly resistant to the etch chemistries studied. Post-process, all samples were rinsed in methanol and/or acetone to remove the mask material, then rinsed with water and dried with compressed air. Etch rates and feature evolution were determined by scanning electron microscopy (SEM) analysis or stylus profilometry. For the $Ar/SF_6$ mixtures, photoresist patterned wafers were used but were found to be incompatible with the etch chemistry, as large quantities of debris formed on the sample's

surface. It was later learned that the patterned resist mask had not been fully developed and cleaned, resulting in unwanted deposits on the sample.

While the silver print epoxy worked reasonably well as a mask for the $SF_6$ based chemistries studied, extremely sloped features were still seen. When sub-micron alumina dust was added to the silver print mask for additional chemical resistance, sub-micron features with straighter sidewalls were seen. Figure 1 shows both of these features: the gently sloped interface between the masked and unmasked surfaces superimposed on well-defined pillars formed by a few particles of alumina hard mask (the mask material has been removed).

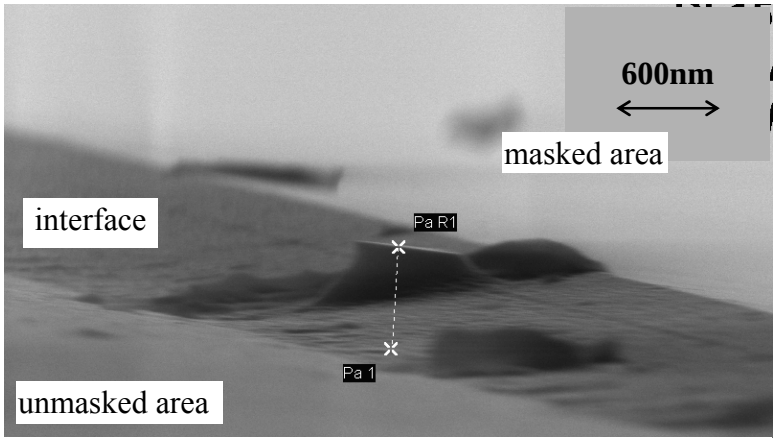


**Figure 1 SEM of silver mask edge where a sloped interface superimposed on alumina micro-masked features formed, showing the different sidewall evolution. Etch conditions were 65 mtorr Ar/5 mtorr $SF_6$ and –100 $V_{bias}$.**

## 3. ETCHING DATA

A listing of all individual etches with all experimental settings and readings are given in Appendix A, in Excel spreadsheet format. Etch chemistries studied were $Ar/SF_6$ and $O_2/SF_6$ mixtures with brief studies on ion energy dependence. No duty factor dependencies were investigated. Etch rates were determined on silicon pieces masked with silver print epoxy. Etch depths on the $O_2/SF_6$ samples were measured using a Tencor (P-10) profilometer, and SEM analyses was used in the $Ar/SF_6$ samples. All errors shown in etch rate are from multiple etch depth determinations on single samples.

Etch rates are calculated using the rf-exposure time to the plasma, not [the] laboratory time.

### *3.1. $O_2/SF_6$ Chemistries*

Mixtures of $O_2$ and $SF_6$ were initially studied to look at the formation of negative ions in these plasmas. The work being discussed here focuses on the application of these plasmas for etching. When a small amount of $SF_6$ was added to a pure $O_2$ plasma, the coupling of rf power to the processing stage changed dramatically as shown in Fig 2.[12] In a pure $O_2$ plasma (Fig 2(a)), the rf power to the stage sustained a secondary discharge well after the 500 μs e-beam pulse, specifically for the duration of the applied rf voltage (purposely lengthened to 1.25 ms to illustrate these changes). In Fig 2(b), the effect due to $SF_6$ addition is shown. Now the secondary discharge in this mixture is not sustained – the dc level of the voltage drops to zero once the e-beam goes off. With a constant rf power applied, the peak-to-peak rf voltages and dc bias level decreased significantly, with even small amounts of $SF_6$ in the mixture.[13] Alternatively, 30% more power[14] was required to achieve the same rf bias level of –100 V, with the same match box setting.

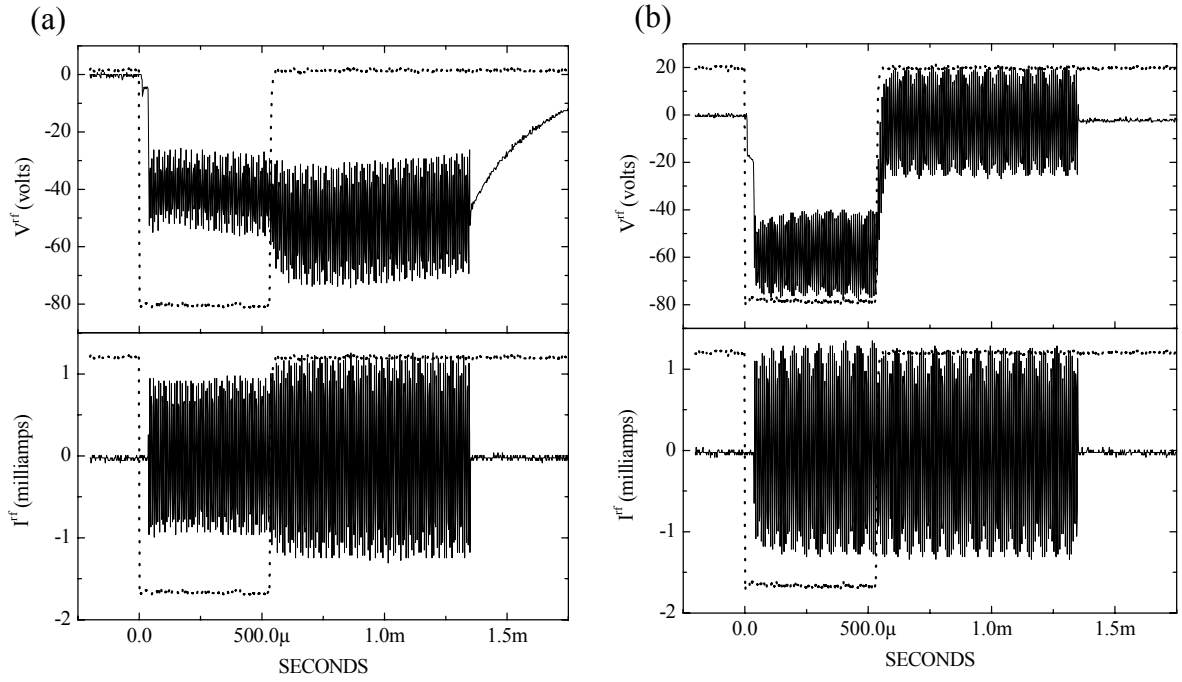


**Figure 2 Rf voltage and current measured on stage at external pick-off box for (a) pure $O_2$ plasma and (b) $O_2$ plasma with 5 mtorr $SF_6$. (The applied rf power was greater in (b).) The dotted lines show the e-beam voltage pulse.**

### *3.1.1. Etch rate with respect to rf bias*

The etch rate with respect to the rf bias ($V_{bias}$) for the plasma operating with 15 mtorr $SF_6$ in 45 mtorr $O_2$ is shown in Fig 3. The dependence was weaker than linear and the etch rate reached a maximum of 960 Angstroms/minute at –200 V bias. Magnetic field strength was 90 Gauss, and the cathode was operating at standard conditions of a –2 kV/ 2 ms pulse at a repetition rate of 50 Hz.

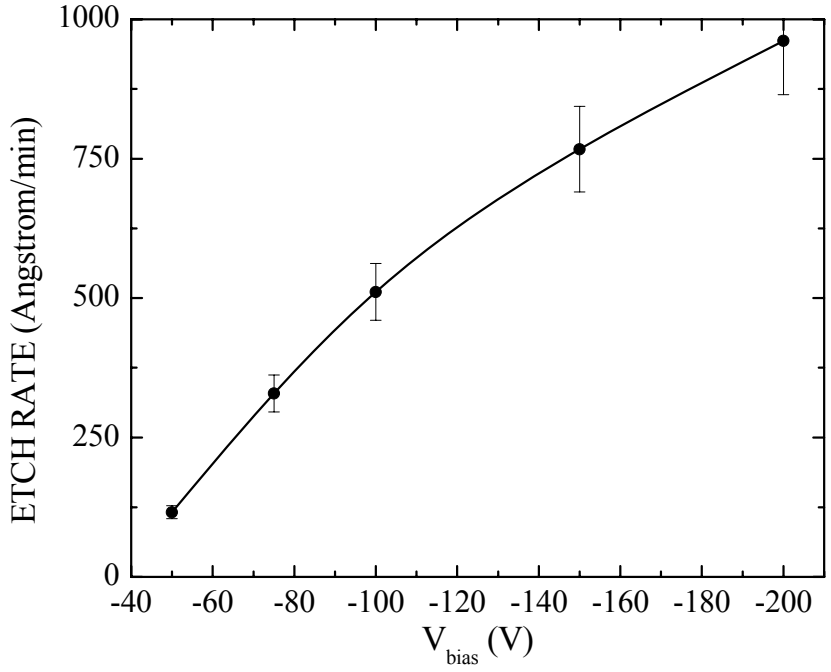


**Figure 3 Etch rate vs $V_{bias}$ for 45 mtorr $O_2$/15 mtorr $SF_6$ mixtures.**

### *3.2. Ar/$SF_6$ Chemistries*

Like the $O_2/SF_6$ mixtures, the $Ar/SF_6$ mixtures were also studied to look at the formation of negative ions. The coupling of rf power to the processing stage was slightly different[15] than in the $O_2/SF_6$ mixtures. In the $Ar/SF_6$ mixtures, ion fluxes to a stage were also measured[16] with a mass spectrometer (Hiden EQP300), and typical spectra are shown in Fig 4. In these experiments, the gas mixture contained a 50/50 mix of $Ar/SF_6$. With small dc voltage levels (±8 Vdc) applied to the sampling stage, large quantities of both positive and negative ions were detected during the active (beam on) phase of

plasma production. The positive ion spectrum (4a) was dominated by $SF_5^+$, followed by $Ar^+$ then $SF_3^+$. The negative ion spectrum (4b) was dominated by $SF_6^-$ followed by $SF_5^-$ then $F^-$. These spectra are considered examples, in that they strongly depend on the conditions[i] at which they were collected.[17] For the gas mixtures used in these etching experiments, the dominant positive ion species were $SF_5^+$, $SF_3^+$ and $Ar^+$, respectively, however no negative ion species were detected at the applied (±8 V) voltages.

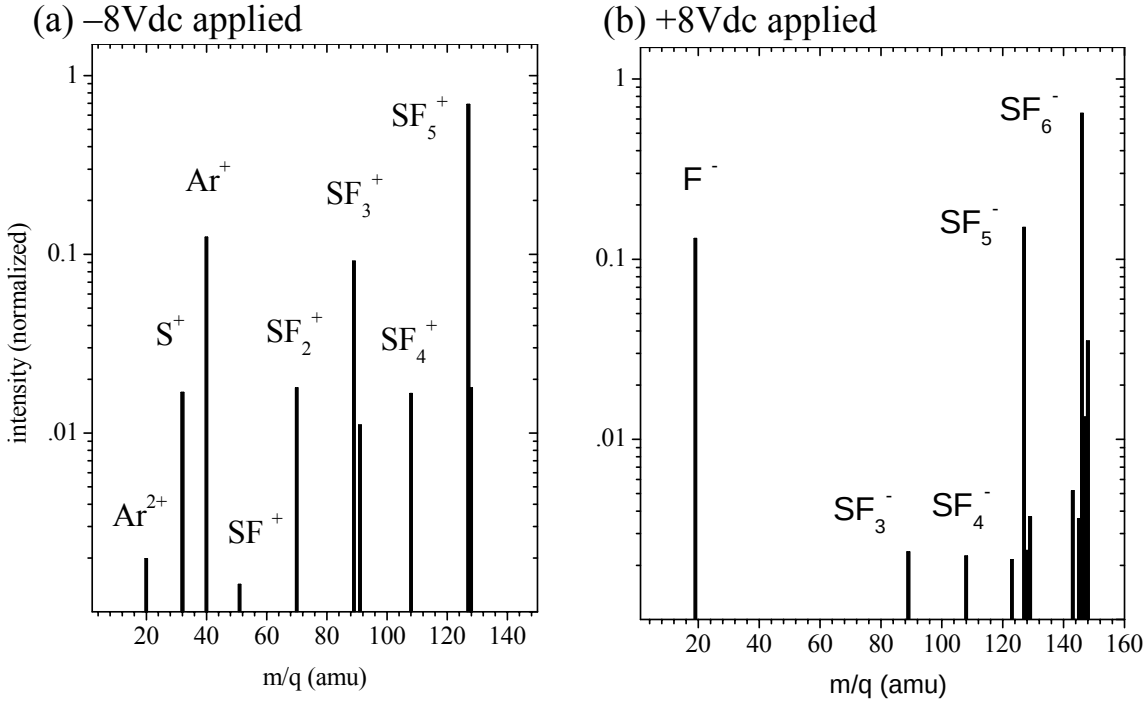


**Figure 4 Mass spectrum of (a) cations and (b) anions drawn to biased electrode for a 50 mtorr Ar/50 mtorr $SF_6$ mixture.**

### *3.2.1. Etch rate with respect to rf bias*

The silicon etch rate with respect to rf bias is shown in Fig 5. The gas mixture was fixed at 50 mtorr argon and 20 mtorr $SF_6$. Typical processing times were 1-2 minutes. As seen in Fig 5, the etch rate was more linear than the analogous $O_2/SF_6$ mixtures and nearly an order of magnitude larger.

[i] For these spectra, the energy analyzer was set at a fixed passband. In the positive ion spectrum, the passband was centered at the peak of the $Ar^+$ energy distribution while the negative ion spectrum was based on the $F^-$ energy distribution.

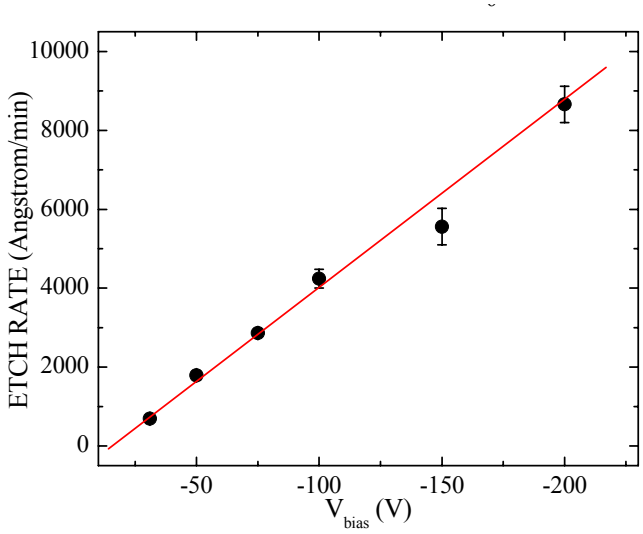


**Figure 5 Etch rate vs $V_{bias}$ for 50 mtorr Ar/20 mtorr $SF_6$ mixture**

### *3.2.2. Etch rate with respect to gas mixture*

The etch rate of silicon with respect to $SF_6$ partial pressure in argon is shown in Fig 6. The rf bias level and total pressure were held constant (–100 V and 70 mtorr, respectively). Changes in plasma density with gas composition were not measured. Figs 7(a) and (b) show SEM photographs of micron-sized features for the 15% and 45% $SF_6$ in argon mixtures.

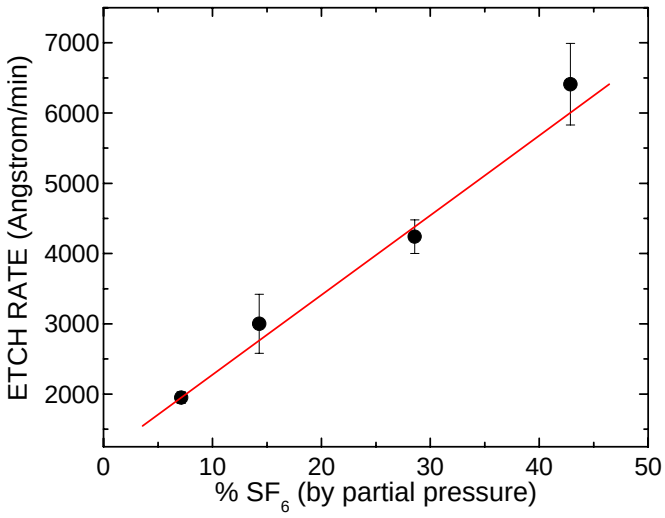


**Figure 6 Etch rate vs $SF_6$ percentage on Ar/$SF_6$ mixtures**

(a)

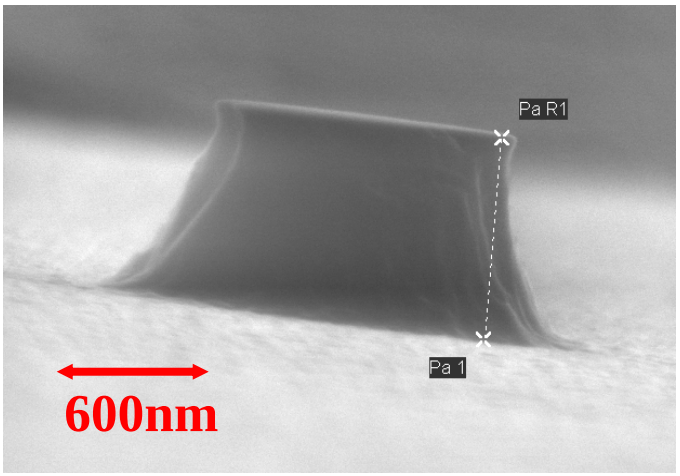


(b)

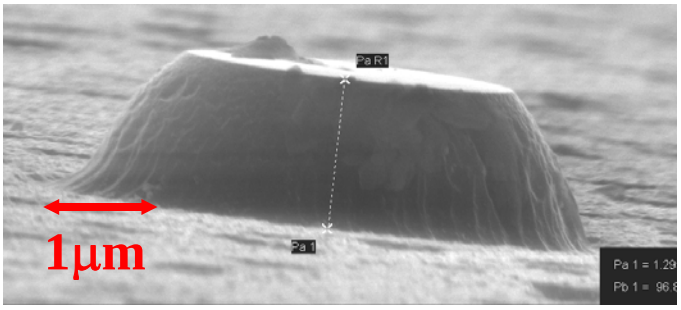


**Figure 7 SEM photographs of Ar/$SF_6$ mixtures containing (a) 15% and (b) 45% $SF_6$ by partial pressure. Rf bias level was fixed at –100 V.**

## 4. RESULTS AND DISCUSSION

### *4.1. Stage Characteristics and Rf Biasing of Stage*

The general characteristics of coupling an rf biased stage to LAPPS has been discussed in detail elsewhere.[10] It is important to reiterate here that the signals measured [at the rf pick-off box] are not necessarily the signals at the stage surface, but serve as a guide for coupling the rf power through the stage to the plasma and the day-to-day reproducibility. It should also be pointed out that the peak-to-peak voltages and currents listed in Tables I and II were not necessarily in phase. Thus, the actual power being applied is not merely the product of the current and voltage, but must be multiplied by the cosine of the phase between the two signals. Such measurements were not the focus of these experiments, and the data is reported only as a guide for future experiments.

The stage performed differently in the acrylic chamber, where a persistent negative dc voltage was seen without any rf being applied, even with pure gases (Ar and $O_2$). This

negative voltage discussed in Section 2.2 can be seen in the top traces of Fig 2, immediately before the rf is applied. Although the offset signal for the pure $O_2$ case (Fig 2(a)) was approximately –5 V, the addition of $SF_6$ (Fig 2(b)) causes a significant increase to –18 V. These offset signals continued through the entire beam pulse and were strongly dependent on gas composition. They are believed to be the result of uncontrollable process conditions such as wall conditioning and contamination. Specifically, plasma products (radicals, UV light, ions) react with the chamber walls forming volatile compounds, which can then further react and deposit on the stage. These deposits form a thin [semi-insulating] dielectric on the stage surface. The addition of $SF_6$ clearly expedites these wall reactions, thereby increasing the charge build-up on the stage. Similar surface [charging] effects were seen with inductively coupled discharges containing $SF_6$, which resulted in strong shifts in the ion energy distributions.[18] In those experiments, which were carried out in a stainless steel chamber using a grounded stage, a bluish film was also observed on the front of the stage, believed to "possibly be a polymeric coating of much lower conductivity."

When the stage was placed in the metal chamber, the primary deposition source (the acrylic wall) was eliminated and the plasma was able to clean previous deposits re-establish a reasonable potential. An additional experiment to artificially re-create this effect using dielectric films proved to be uninformative and was not pursued as a focus of research.

### *4.2. Etching*

The deposition of the dielectric film previously discussed can significantly skew etch conditions. In these experiments, it was believed that the major effect was the improper representation of the rf bias level due to surface charging as illustrated in Fig 2. The dc offset from surface charging was approximately –20 V, which was included in the rf bias ($V_{bias}$) measurement. Therefore the actual rf bias on the stage should be the reported $V_{bias}$ value, less the 20 V dc signal from surface charging. Nonetheless, the reported $V_{bias}$ values in Figs 3, 5 and 6 are representative of the incident ion energy.

Although not emphasized in these experiments, the effect of duty factor should also be considered. References cited in the literature used continuous plasma sources,

whereas the experiments reported here were a pulsed source. The large off-time between pulses left ample time for deposition and further reactions of thick 'selvedge' and/or capping layers. Also, at these low duty factors all plasma species should have completely decayed away before the next plasma pulse, so a duty factor dependence would not be expected. Higher duty factor studies could show if there is a re-initialization of the etch process at the start of every plasma pulse and could thereby determine the effects of deposition processes. While a more in-depth analysis of surface composition would be useful, the film deposition did not appear to be a physical barrier (i.e. etch stop) in the removal of silicon from the present SEM studies.

### *4.2.1. $O_2/SF_6$ mixtures*

The etch rate (ER) of silicon was fairly low in these $O_2/SF_6$ mixtures, reaching a maximum at ~ 1000 Å/min at the maximum ion energy of –200 V. This low etch rate could be due to any of the following: redeposition or growth of $SiO_x(F_y)$ complexes[i] on the surface, deposition of $SF_x$ intermediates and/or low plasma density. If we make the reasonable assumption that the ion densities are comparable in the etching tests, then the changes seen are due to the competition between deposition and evolution of volatile etch products. In a general etching environment, the formation of oxides (or oxyfluorides) on exposed silicon can quench chemical etching. In fact, such passivating layers are considered the key to anisotropic pattern transfer for such chemistries. Since the formation of the passivating layers has been discussed in the scientific literature and should apply in LAPPS, a comparison of plasma formation and plasma chemistry is in order.

Conventional plasma sources are driven by electric fields which heat plasma electrons to reach the lowest gas ionization potential and sustain the discharge. At energies below the ionization and dissociation threshold, inelastic collisions dominate, causing the energy that is put into them to be largely wasted. This is an inefficient use of power since (1) only a small portion of the plasma electron distribution actually ionizes the gas and (2) the electrons are constantly heated from room temperature to maintain

[i] Since there was no definitive identification of the passivation layer, the formula $SiO_x(F_y)$ is used to represent either $SiO_x$ of $SiO_xF_y$ compounds.

ionization, thereby constantly driving the $SiO_x(F_y)$ low-energy reactions. Since dissociation[i] cross sections mimic ionization (except for lower threshold energies), conventional discharges are similarly inefficient at gas dissociation. Furthermore, the strong dependence of gas ionization and dissociation rates with electron temperature can thus produce large changes in the plasma chemistry and subsequent etch rates. In conventional sources with $O_2/SF_6$ chemistries, silicon etch rates have been reported from 0.2 to 3 microns/min[ii] and are relatively uncorrelated to $O_2$ percentage. In LAPPS, a high-energy electron beam initiates gas ionization. This means that nearly *all* electron-induced reactions are available, depending on their cross section, with high-energy (i.e. ionizing) collisions occurring first. The secondary (plasma) electron distribution is cooled to below 1 eV[iii] by additional collisions with the background gas, if necessary. There is no churning of the low energy reactions as in a conventional discharge.

For $O_2$ and $SF_6$, major electron-driven processes (ignoring vibrational excitations) are shown in Figs 8 and 9, respectively. The $O_2$ cross sections are well represented here but the caveats[19] associated with the $SF_6$ cross sections must be noted. First, certain electronic excitations result in dissociative ionization, which is not illustrated in Fig 9. Thus, an *additional* ionization cross section should be considered, with a magnitude and dependence similar to the total ionization cross section. Second, ionization itself is dissociative, with $SF_5^+$ being the largest ion formed.[20] Finally, like other large fluorinated molecules, all electronic excitations lead to dissociation of the molecule. Hence, there is far more molecular fragmentation than Fig 9 implies at first glance. Production of the major etchant, atomic fluorine, can therefore come from a variety of channels.

Either neutral or ionizing dissociation channels can produce neutral radical species. For oxygen, the gas dissociation mechanism mimics ionization (see Fig 8) as mentioned above. From the cross sections shown in Fig 9, *dissociative attachment*[21] is clearly the dominant dissociation mechanism of $SF_6$ in conventional discharges as well as LAPPS. However, the neutral dissociation reaction rates for specific reactions in the literature are somewhat unclear, ranging from the 58 $s^{-1}$ rate quoted in Section 1.1 for the reaction $SF_6$

[i] This does not include dissociative attachment.
[ii] Oxygen concentrations and etch rates quoted here are from a variety of papers and plasma sources.
[iii] Here, molecular gases are being considered.

+ $e^- \rightarrow SF_2 + 4F + e^-$ to less than 20 $s^{-1}$ at 1 Torr.[22] A similar dissociation pathway has also been reported[23] for a capacitive discharge operating at lower pressures (20-200 mtorr): $SF_6 + e^- \rightarrow SF_4 + 2F + e^-$ with a dissociation rate of $k_d \sim 700\ s^{-1}$. These rates must equal the product of the target density ($N(SF_6)$) multiplied by the volumetric rate coefficient ($<\sigma v>$) which can then be compared to the cross section in Fig 9. However, the rate coefficient ($k_d$) is expected to vary as $\exp(-W_d/T_e)$ where $T_e$ is the electron temperature and $W_d$ is the threshold energy. Assuming an electron temperature of a few electron volts and $W_d \sim 10$ eV (from Fig 9), the exponential term is indeed an important factor. An approximate calculation [$N\sigma v \sim k_d \exp(-W_d/T_e)$] given the pressures involved and $T_e = 1$eV (thereby maximizing the exponential dependence) yields a cross section of $10^{-16}$–$10^{-19}$ $cm^2$ for the lowest and highest pressures, respectively. It would appear that the collective dissociation cross section illustrated in Fig 9 is over-represented or these reaction rates are under estimated.

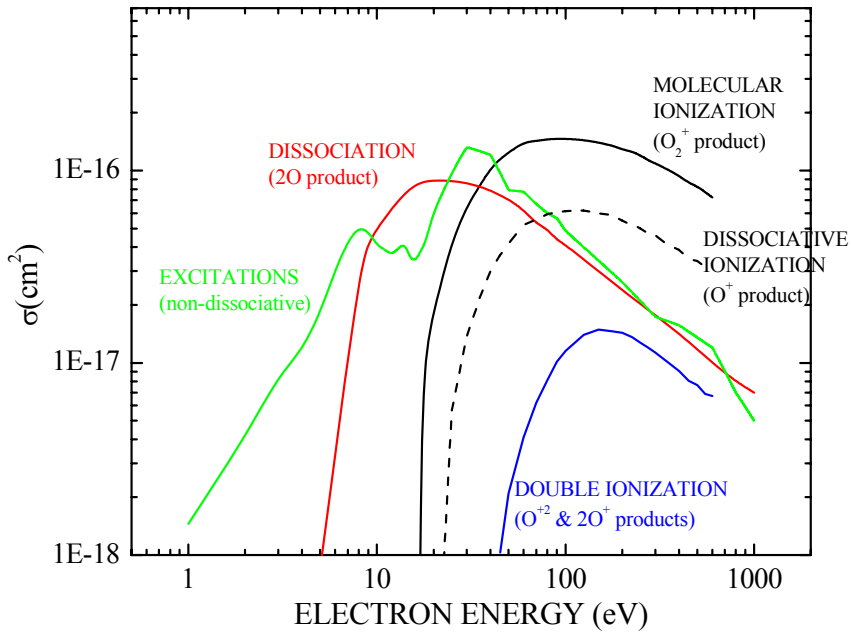


**Figure 8 Electron collision cross sections for $O_2$.**

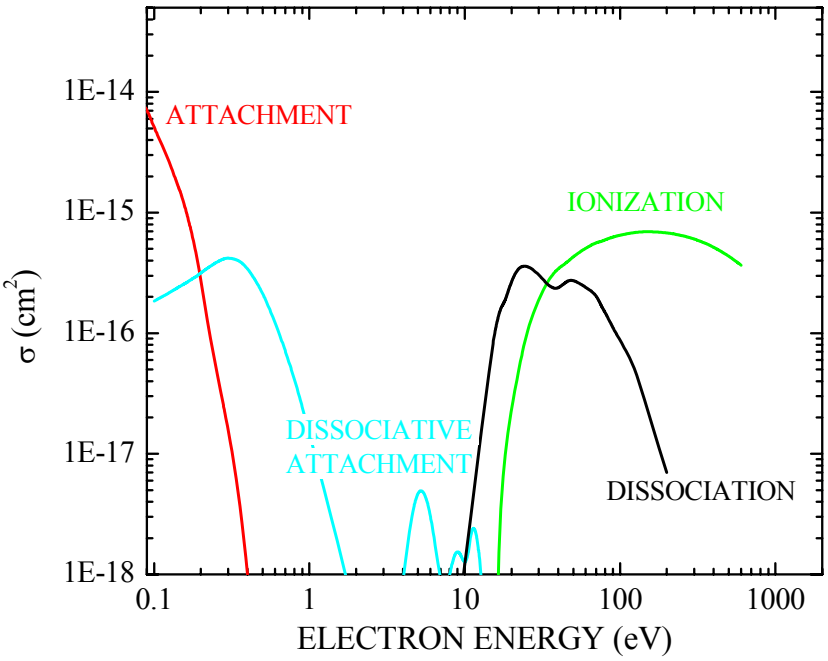


**Figure 9 Electron collision cross sections for $SF_6$.**

Reactive ion etching also relies on the composition of ion species to the surface for material removal. In oxygen, electron beams produce significantly more atomic ions than conventional discharges, possibly at the expense of neutral atom production. In $SF_6$, gas ionization results in free radicals, which is true regardless of the plasma source. However, the energetic electron beam initially creates[20] the ion $SF_5^+$ (and then $SF_3^+$). In conventional discharges the low-energy electrons break up the molecules first through dissociative attachment and then ionize the molecular fragments. This can be confirmed experimentally, by comparing the data in Fig 4 with the work of the NIST group which show in conventional inductive[24] and capacitively[25] coupled discharges, the flux of $SF_3^+$ and the flux of $S^+$ are the dominant species, respectively. Of course, ion-molecule reactions also occur in all of these mass spectrometry measurements. The reaction $SF_5^+ + SF_6 \rightarrow SF_3^+ + SF_6 + F_2$ has an appreciable rate at low energies[26,27] and is considered to be responsible for the dominance of $SF_3^+$ in the capacitively coupled discharge experiments. However in LAPPS, which has even lower ion energies,[17] $SF_5^+$ remained the dominant ion.[28] This comparison would imply that the capacitive discharge is actually breaking up the $SF_6$ molecule more than was realized, or the charge exchange cross section has a

strong dependence on ion energy. When oxygen is included, the atomic ions (which are abundant in LAPPS) can dissociatively charge transfer through the reaction ($O^+ + SF_6 \rightarrow SF_5^+ + FO$), to make a more massive reactive ion. Although the reactive fluorine atom is lost through this reaction, the flux of reactive $O^+$ is also decreased, which is a potential etch stop species forming $SiO_x(F_y)$ on the surface. The molecular ion is not reactive with $SF_6$ so $O_2^+$ will recombine on the silicon surface. Although ion flux measurements with $O_2/SF_6$ mixtures have not been carried out, such reactions may enhance LAPPS' ability to etch silicon since the dominant ion flux should be the massive sulfur pentafluoride ion, $SF_5^+$.

All of these points imply that LAPPS would be an ideal etch tool with the $O_2/SF_6$ chemistry, which is contrary to the observed low etch rates. This result brings to light two possible conclusions: (1) LAPPS also has ideal conditions to form $SiO_x(F_y)$ on the surfaces, thereby inhibiting the reactive ion etch and (2) the incident ion energies were not high enough to remove the $SiO_x(F_y)$ passivating layer. The second point somewhat follows the first, and has the obvious solution of increasing the ion energies. However, if increased ion energies also result in unacceptable surface damage, the first point needs to be fully addressed which means that the gas phase reactions have to be better understood. From the information presented here, some direct assumptions about $SiO_x$ formation can be made: (1) LAPPS operates at moderately high background pressures for an etching reactor, but not extraordinary so, which would rule out the flux of $O_2$ as an issue. (2) The atomic O flux is also plentiful[10], but LAPPS does not produce low-mass $SF_x$ ions, the appropriate getters for the oxygen species. This 'balance' of gas phase species and reactions in LAPPS may be better determined in experiments using varying concentrations of $O_2$ and $SF_6$.

### *4.2.2. Ar/$SF_6$ Mixtures*

The plasma density is typically a factor of 5 higher for pure argon plasmas, while the etch rate was an order of magnitude larger for the $Ar/SF_6$ mixtures in comparison to the $O_2/SF_6$ mixtures. This may have been due, however, to the lack of atomic oxygen species and thus the absence of a capping oxide layer. In the $Ar/SF_6$ chemistry, deposition can only originate from sulfur fluoride compounds, assuming no contaminant

gases.[i] Features due to deposition were visible in all gas mixtures at low ion energies, as shown in Fig 7(a). With $V_{bias} = -100$ V at the lowest percentage of $SF_6$, a small amount of deposition was seen, discernable by the feature's strong anisotropic etch at the top and sidewall sloping around the base. This sloped base may be due to the build up of depositing species in the chamber during the etch. (Note that even though the mask has been removed, an isotropic etch component in these plasma processes would produce an 'hour-glass' profile, which was not seen at anytime in these experiments.) Figure 7(b) from a similarly biased sample in 45% $SF_6$, showed both (1) a strong chemical etching component, with numerous micro-pits on the surface and (2) feature sidewalls which actually bow out, due to a more rapid deposition rate. This implies that a passivating film was growing rapidly during the process, which increased the effective size of the feature. However, this protective film was not impervious to (or possibly contained) a wet chemical component which pooled on the surface and began pitting it. The micropitting implies reactive species are on the surface and sticking for some time, while the feature profile implies a continuous growth of a blocking/passivating layer. Since silicon exposed to a flowing $SF_6$ background showed no spontaneous etching or micropitting, the reaction was indeed driven by plasma-produced F radicals or $F_2$ (from recombination on the surface). While this is reasonable, especially in a pulsed plasma environment (which would be ideal for polymerization as well), the present data is insufficient to make a definitive conclusion. From this data it appears that by varying the duty factor, this etch-deposition cycle could be used to create controllable feature sidewalls and structures.

A blocking layer can also form by plasma species reacting with the mask material (silver print). However, if the resultant silver fluoride (or even silver sulfide) remained on the surface, it is highly insoluble in the solvents used to clean the samples and would therefore be visible on all of the surfaces. The observed features shown in Fig 1 are actually indicative of an eroding mask which was thinner around the edges (like the silver print paint used), given the even slope and sample-to-sample consistency. The fact that the harder alumina particles resulted in more pronounced vertical features also supports the idea that the silver mask was eroding during etching.

[i] This is only approximately true; the chamber base pressure was > $5 \times 10^{-5}$ torr. The wall reactions discussed earlier are similarly a contributing factor.

The wide range of positive ions shown in Fig 4(a), suggests that ion-molecule reactions could be important in these mixtures as well. Argon ionization has a threshold energy of 15.75 eV, while the ionization threshold for $SF_6$ is very similar[29] (15.3-15.8 eV), meaning $Ar^+$ can charge exchange with the more massive molecule, giving up any extra energy to its internal degrees of freedom. This reaction is quite rapid ($k_{ce} \sim 10^{-9}$ $cm^3/s$),[27] producing $SF_5^+ + F$. Hence, the flux of $SF_5^+$ dominates $Ar^+$ for all but the smallest concentrations of $SF_6$.[17] Therefore, even a small amount of $SF_6$ in the gas mixture makes the plasma highly reactive.

### *4.2.3. Negative Ions and Ion-Ion Plasmas*

For the gas compositions used in these etching experiments no negative ions were extracted in the mass spectrometry measurements, which means that an electron-ion plasma was formed. Therefore, the presence of negative ions are not a dominating factor in the etching experiments presented here, but it is still informative to consider the effects of negative ion production and chemistry for future experiments. From Fig 4(b), LAPPS is capable of producing large amounts of negative ions that can be extracted, a character not shared by other plasma sources. This is due to the fact that (1) the electric fields in the plasma are low and more importantly, (2) the cold plasma electrons are not constantly heated to drive gas ionization but are a byproduct of it. The dominance of the $SF_6^-$ species confirms the attachment of extremely low energy electrons (< 0.5 eV) while the $SF_5^-$ and $F^-$ are created by dissociative attachment with higher energy electrons.[7]

Previous studies (see References 8, 9 and 30) had concluded that negative ions could be used to reduce surface charging and also etch material, with an appropriate bias signal applied to the etching stage. The primary limitation in those experiments was that the negative ion fluxes were confined to a short fraction of the afterglow, because of the high electron temperature during the discharge period. As shown in Fig 4, these limitations have been largely removed in LAPPS and therefore a truly bipolar-ion etching arrangement could be realized, given that comparable amounts of positive and negative ions can be extracted. By applying a low frequency (2-150 kHz) potential to the stage, the ions will be able to respond while the average (dc) voltage remains near zero. The

positive effects of negative ions have not yet been exploited and are presently an area of active research.

## 5. SUMMARY

An e-beam produced plasma sheet (22 x 30 x 1cm$^3$) was used to etch <110> silicon. A pulsed hollow cathode source operated at 2 keV in a uniform 80-90 Gauss magnetic field was used to supply the e-beam. Gas compositions consisted of 45 mtorr $O_2$ with 15 mtorr $SF_6$, and Ar mixtures with 5-40% of $SF_6$. A large disparity in etch rate was observed for these mixtures, with the etch rate in $O_2$ roughly 10 times slower than in argon. At maximum ion energies studied here (-200 V), the $O_2/SF_6$ mixture reached a maximum etch rate of 1000 Å/min while the $Ar/SF_6$ mixture had an etch rate of ≈ 10,000 Å/min. There was strong competition between the deposition and etching processes in both plasma chemistries studied, which led to the different etch rates. It was hypothesized that when oxygen was in the gas mixture, an involatile $SiO_xF_y$ capping layer was able to form, while oxygen-free mixtures resulted in more penetrable $SF_x$ passivating films. These deposition processes could possibly be controlled to tailor feature profiles by investigating the effects of duty factor on feature evolution.

Based on a description of plasma chemistry, insight into the prospects of LAPPS in these gas mixtures was discussed. Both positive and negative ion chemistries favor larger bulky molecular ions, specifically $SF_5^{+/-}$ as opposed to conventional discharges which tend to dissociate large molecules and create lower molecular weight ions. The use of LAPPS as a bipolar-ion etching source to minimize damage due to surface charging is considered promising and only now being explored.

## 6. CONCLUSION

LAPPS has been shown to etch silicon at room temperature without significant undercutting of large (multiple micron) features. The redeposition of species during plasma on and off times can be a help or a hindrance to feature profiles. The differences in plasma chemistry between $O_2/SF_6$ and $Ar/SF_6$ are now fairly well understood. A robust ($SiO_2$) mask would be a good test of these hypotheses. The attributes of negative ions in LAPPS opens possibilities not available in conventional plasma sources.

ACKNOWLEDGEMENTS

This work has been supported by the Office of Naval Research. The authors gratefully acknowledge the technical support of Mr. Anthony Noll and Robert Lanham, of NRL and SFA, Inc., respectively.

# APPENDIX A

## Detailed information of individual etches.

## BASICS

| SAMPLE # | DATE RUN | DUTY FACTOR (%) | POSITION (mm from beam edge) | GAS PRESSURE | PROCESS TIME (min) | Vrfidcb (V) | ETCH RATE (nm/min) | COMMENTS |
|---|---|---|---|---|---|---|---|---|
| DL10-116-Si | 10/16/01 | 10 | ~5 | 45/15 mT O2/SF6 | >5 | -100 | >38.5 | plexi chamber; alot of monkeying around with rf stage and coupling |
| DL10-120-Si | 10/19/01 | 10 | ~5 | 45/15 mT O2/SF6 | 15 | -100 | 51.1 | plexi chamber; clean run; stage may not have been in identical plase as in DL10-116 run |
| DL10-122-Si | 10/22/01 | 10 | ~5 | 45/15 mT O2/SF6 | 12 | -150 | 76.7 | plexi chamber; clean run; |
| DL10-124-Si | 10/23/01 | 10 | ~5 | 45/15 mT O2/SF6 | 12 | -50 | 11.6 | plexi chamber; clean run; changed stage to accomodate cartridge loading; simultaneously ran 'chemical only' sample which showed no etching |
| DL10-126-Si | 10/24/01 | 10 | ~5 | 45/15 mT O2/SF6 | 12 | -75 | 32.9 | plexi chamber; clean run; |
| DL10-127-Si | 10/25/01 | 10 | ~5 | 45/15 mT O2/SF6 | 9 | -200 | 96.1 | plexi chamber; clean run; used PR mask |
| DL15-16-J | 1/13/02 | 10 | ~5 | 53mT O2? | 6 | -75 | 166 | plexi chamber; clean run but rf bias erratic |
| DL15-18-L | 1/14/02 | 10 | ~5 | 42/17mT O2/SF6 | 6 | -50 | 63 | plexi chamber; attempted to put initially tried to put + bias on stage for - ions; many issues with this run |
| DL15-67-Si | 5/13/02 | 10 | ~5 | 60/20mT Ar/SF6 | 2 | -50 | 191 | plexi chamber; no problems; 180 Gauss |
| DL15-71-M | 5/14/02 | 10 | ~5 | 50/20mT Ar/SF6 | 1 | -100 | 424 | plexi chamber; no problems; 180 Gauss |
| DL15-75-N | 5/15/02 | 10 | ~5 | 51/20mT Ar/SF6 | 1 | -150 | 556 | plexi chamber; no problems; 180 Gauss |
| DL15-77-O | 5/15/02 | 10 | ~5 | 50/19mT Ar/SF6 | 1 | -75 | 286 | plexi chamber; no problems; 180 Gauss |
| DL15-83-P | 5/16/02 | 10 | ~5 | 52/20mT Ar/SF6 | 4 | -75 | 179/75 | retry of DL15-77; lengthened exposure time |
| DL15-88-Q | 5/20/02 | 10 | ~5 | 65/5 mT Ar/SF6 | 1 | -100 | 650 | plexi chamber; no problems; 180 Gauss |
| DL15-95-Si | 5/21/02 | 10 | ~5 | 60/10 mT Ar/SF6 | 1 | -100 | 301 | plexi chamber; no problems but had replaced turbo prior to run; 180 Gauss |
| DL15-97-Si | 5/22/02 | 10 | ~5 | 65/5 mT Ar/SF6 | 3 | -100 | 195 | rerun of DL15-88 for longer time |
| DL15-101-Si | 5/22/02 | 10 | ~5 | 50/20mT Ar/SF6 | 2 | -100 | 429 | plexi chamber; no problems; 180 Gauss |
| DL15-103-Si | 5/23/02 | 10 | ~5 | 49/20 mT Ar/SF6 | 4 | -32 | 69 | plexi chamber; no probs; 180 Gauss |
| DL15-105-Si | 5/23/02 | 10 | ~5 | 50/20 mT Ar/SF6 | 1 | -200 | 872 | plexi chamber; no probs; 180 Gauss |
| DL15-109-Si | 5/23/02 | 10 | ~5 | 39/30 mT Ar/SF6 | 2 | -100 | 641 | plexi chamber; no probs; 180 Gauss |

CATHODE

| SAMPLE # | CHAMBER BASE PRESSURE | V/r | PULSE LENGTH (ms) | REP RATE (Hz) | DUTY FACTOR (%) |
|---|---|---|---|---|---|
| DL10-116-Si | 0 mT | 2 | 5 | 20 | 10 |
| DL10-120-Si | 0 mT | 2 | 5 | 20 | 10 |
| DL10-122-Si | 0 mT | 2 | 5 | 20 | 10 |
| DL10-124-Si | 0 mT | 2 | 5 | 20 | 10 |
| DL10-126-Si | 0 mT | 2 | 5 | 20 | 10 |
| DL10-127-Si | 0 mT | 2 | 5 | 20 | 10 |
| DL15-16-J | 0 mT | -9.6 | 0.5 | 200 | 10 |
| DL15-18-L | 0 mT | -9.6 | 0.5 | 200 | 10 |
| DL15-67-Si | 0 mT | -9.25 | 2 | 50 | 10 |
| DL15-71-M | 0 mT | n/a | 2 | 50 | 10 |
| DL15-75-N | 0 mT | n/a | 2 | 50 | 10 |
| DL15-77-O | 0 mT | -9.5 | 2 | 50 | 10 |
| DL15-83-P | 0 mT | -9.9 | 2 | 50 | 10 |
| DL15-88-Q | 0 mT | -9.5 | 2 | 50 | 10 |
| DL15-95-Si | 0 mT | -9.5 | 2 | 50 | 10 |
| DL15-97-Si | 0 mT | -9.5 | 2 | 50 | 10 |
| DL15-101-Si | 0 mT | -9.4 | 2 | 50 | 10 |
| DL15-103-Si | 0 mT | -9.6 | 2 | 50 | 10 |
| DL15-105-Si | 0 mT | -9.5 | 2 | 50 | 10 |
| DL15-109-Si | 0 mT | -9.4 | 2 | 50 | 10 |

RF INFORMATION

| SAMPLE # | Vpp (volts) | Ipp (amps) | L/T | Tmax |
|---|---|---|---|---|
| 001012A (DL10-53) | 201 | 5.08 | | 34 |
| DL10-116-Si | 79 | 5.37 | 0.30/0.30 | n/a |
| DL10-120-Si | 77 | 5.82 | 0.30/0.30 | n/a |
| DL10-122-Si | 117 | 7.85 | 0.40/0.20 | n/a |
| DL10-124-Si | 38 | 2.74 | 0.40/0.20 | n/a |
| DL10-126-Si | 56 | 4.05 | 0.45/0.25 | n/a |
| DL10-127-Si | 156 | 9.72 | 0.50/0.20 | n/a |
| DL15-16-J | 43-67 | 3.6 | 0.50/0.15 | n/a |
| DL15-18-L | 25 | 1.3 | 0.50/0.15 | n/a |
| DL15-67-Si | 60 | 2.1 | 0.55/0.30 | n/a |
| DL15-71-M | 130 | 3.86 | 0.60/0.30 | n/a |
| DL15-75-N | 199 | 6.07 | 0.40/0.30 | n/a |
| DL15-77-O | 91.7 | 2.84 | 0.45/0.30 | n/a |
| DL15-83-P | 55 | 1.73 | 0.40/0.28 | n/a |
| DL15-88-Q | 135 | 3.99 | 0.60/0.28 | n/a |
| DL15-95-Si | 135 | 4.04 | 0.48/0.30 | n/a |
| DL15-97-Si | 128 | 3.84 | 0.60/0.25 | n/a |
| DL15-101-Si | 141 | 4.3 | 0.60/0.32 | n/a |
| DL15-103-Si | 17.8 | 0.54 | 0.60/0.32 | n/a |
| DL15-105-Si | 272 | 8.09 | 0.50/0.32 | n/a |
| DL15-109-Si | 63.1 | 2.87 | 0.55/0.35 | n/a |

SURFACE

| SAMPLE # | SEM/profilometry |
|---|---|
| DL10-116-Si | 0.5 micron step from Ag print mask |
| DL10-120-Si | 0.826 micron step from Ag print mask |
| DL10-122-Si | 0.920 micron step from Ag print mask |
| DL10-124-Si | 0.1389 micron step from Ag print mask |
| DL10-126-Si | 0.395 micron step from Ag print mask |
| DL10-127-Si | micron step from Ag print mask |
| DL15-16-J | PR patterned sample; SEM showed undercuting |
| DL15-18-L | PR patterned sample; SEM shows severe undercutting; poor photos |
| DL15-67-Si | both PR patterned and bulk Si samples; debris EVERYWHERE on patterned sample. Stepwise feature evolution seen also |
| DL15-71-M | both PR patterned and bulk Si samples; debris AWFUL on patterned sample. |
| DL15-75-N | patterned and bulk samplerun; SEM shows less debris; broke bulk sample |
| DL15-77-O | patterned sample showed no material removal; bulk sample showed step; clearly redepositing on PR patterned piece (only?!) |
| DL15-83-P | patterned sample showed minimal material removal and heavy debris; bulk sample showed larger step; clearly redepositing on PR patterned piece |
| DL15-88-Q | patterned sample showed smaller material removal and heavy debris; bulk sample showed larger step, from booger; |
| DL15-95-Si | bulk Si with 'dust' as mask (unsuccessful); Surface looks decent |
| DL15-97-Si | bulk Si with 'dust' as mask; Surface looks decent but varying etch depths, presumably due to mask erosion |
| DL15-101-Si | bulk Si with 'dust' as mask; Surface looks poor |
| DL15-103-Si | bulk Si with Ag print mask; Surface OK |
| DL15-105-Si | bulk Si with Ag print mask; Surface good - looks like masked areas |
| DL15-109-Si | bulk Si with Ag print mask; Surface good |

## REFERENCES


[1] Plasma Etching: An Introduction, D.M. Manos and D.L. Flamm, eds.(New York: Academic Press, 1989).
[2] A.A. Ayón, R. Braff, C.C. Lin, H.H. Sawin and M.A. Schmidt, *J. Electron. Mat.* **146**, 339 (1999). This paper introduces the 'time-multiplexed deep etching (TMDE)' technique which is an extensive study of the Bosch process. See references within for details.
[3] I. Hassan, C.A. Pawlowicz, L.P. Berndt and N.G. Tarr, *JVSTA* **20**, 983 (2002).
[4] M. Zhang, J.Z. Li, I. Adesida and E.D. Wolf, *JVSTB* **1**, 1037 (1983).
[5] H. Jansen, M. de Boer, R. Legtenberg and M. Elwenpoek, *J. Micromech. Microeng.* **5**, 115 (1995).
[6] D. Leonhardt, S.G. Walton, D.D. Blackwell, W.E. Amatucci, D.P. Murphy, R.F. Fernsler and R.A. Meger, *J. Vac. Sci. Technol. A* **19**, 1367 (2001).
[7] L.E. Kline, D.K. Davies, C.L. Chen and P.J. Chantry, *J. Appl. Phys.* **50**, 6789 (1979).
[8] S. Samukawa and T. Mieno, *Plasma Sources Sci. Technol.* **5**, 132 (1996).
[9] T. Shibayama, H. Shindo and Y. Horiike, *Plasma Sources Sci. Technol.* **5**, 254 (1996).
[10] D. Leonhardt, S.G. Walton, D.D. Blackwell, D.P. Murphy, R.F. Fernsler and R.A. Meger, "Photoresist removal in LAPPS," NRL Memorandum Report NRL/MR/6750--S02-8649..
[11] D. Leonhardt, "Parallel wall shielded hollow cathode in plexiglass chamber," NRL Code 6752 informal technical note, 11 July 1999.
[12] See experiments on DL15-21.
[13] In a pure $O_2$ plasma, $<V^{rf}>\sim$ -100V when $V^{rf}_{pp}$ was 150V. With the addition of $SF_6$, $<V^{rf}>\sim$ -150V was achieved when $V^{rf}_{pp}$ was 117V. See experiments on DL10-122.
[14] See experiments on DL10-115.
[15] In a pure Ar plasma, $<V^{rf}>\sim$ -100V when $V^{rf}_{pp}$ was 150V. With the addition of $SF_6$, $<V^{rf}>\sim$ -100V was achieved when $V^{rf}_{pp}$ was 77V. See experiments on DL10-120.
[16] S.G. Walton, D. Leonhardt, R.F. Fernsler and R.A. Meger, *Appl. Phys. Lett.* **81**, 987 (2002).
[17] S.G. Walton, Proceedings of the SVC 45th Annual Technicial Conference…
[18] R. Forest, J.K. Olthoff, R.J. Van Brunt, E.C. Benck and J.R. Roberts, *Phys. Rev. E* **54**, 1876 (1996).
[19] A.V. Phelps and R.J. Van Brunt, *J. Appl. Phys.* **64**, 4269 (1988).
[20] V.H. Diebler and F.L. Mohler, *J. Res. NBS* **40**, 25 (1948).
[21] R. d'Agostino and D.L. Flamm, *J. Appl. Phys.* **52**, 162 (1981).
[22] K.R. Ryan and I.C. Plumb, *Plasma Chemistry and Plasma Processing* **10**, 207 (1990).
[23] A. Picard, G. Turban and B. Grolleau, *J. Phys. D* **19**, 991 (1986).
[24] A.N. Goyete, Y. Wang and J.K Olthoff, *J. Vac. Sci. Technol. A* **19**, 1294 (2001).
[25] R. Forest, J.K. Olthoff, R.J. Van Brunt, E.C. Benck and J.R. Roberts, *Phys. Rev. E* **54**, 1876 (1996).
[26] Z.A. Talib and M. Saporoschenko, *Int. J. Mass Spectrom. Ion Processes.* **116**, 1 (1992).
[27] K. Bederski and L Wójcik, *Int. J. Mass Spectrom. Ion Processes.* **154**, 145 (1996).
[28] In fact, as the $SF_6$ concentration was increased in the Ar/$SF_6$ mixtures, the disparity between the $SF_5^+$ and $SF_3^+$ increased as well. See reference 17 for details.
[29] NIST Physical Reference Database located online at http://physics.nist.gov/PhysRefData/contents.html.
[30] S. Kanakasabapathy, M.H. Khater and L.J. Overzet, *Appl. Phys. Lett.* **79**, 1769 (2001).